EMISSIONS INDUCED BY LAND USE AND LAND COVER CHANGE IN THE LEGAL AMAZON FROM REMOTELY SENSED DATA

Patrícia Monique Crivelari-Costa[1], Fernando Saragosa Rossi[2], João Lucas Della-Silva[1], José Wagner de Oliveira-Júnior[3], Newton La Scala Jr[2], Carlos Antonio da Silva Junior[1]

[1]Universidade do Estado de Mato Grosso (UNEMAT), Sinop, Mato Grosso, Brasil, costa.patricia@unemat.br, joao.lucas1@unemat.br, carlosjr@unemat.br; [2]Universidade Estadual Paulista (UNESP), Jaboticabal, São Paulo, Brasil, fernando.rossi@unesp.br, la.scala@unesp.br; [3]Universidade Federal de Mato Grosso (UFMT), Sinop, Mato Grosso, Brasil, jrwagner.9803@gmail.com

ABSTRACT

The Amazon rainforest is a tropical forest and has the greatest biodiversity in the world. Changes in land use and land cover are one of the main factors in the degradation of tropical forests, which contribute to the emission of greenhouse gases. Thus, the objective of this research was to detect the emissions induced by the change of land use and land cover in the Legal Amazon through multispectral images of the MODIS sensor in the period 2009-2019. The land use and land cover data, the gross primary production (GPP) and the flux of carbon dioxide (CO_2flux) were used. The parameters were obtained using JavaScript language as input in the Google Earth Engine platform. CHIRPS dataset was used to ascertain the regularities of precipitation over the time series.

Key words — LULCC, carbon dioxide, Google Earth Engine, remote sensing.

1. INTRODUCTION

The Amazon Forest represents 40% of the global tropical forest area, which corresponds to a third of the planet's humid tropical forests, and comprises the greatest biodiversity in the world [1]. Changes in land use and land cover (LULCC), mainly in tropical forests, contribute significantly to greenhouse gas emissions and play an important role in global climate change [2].

The historical comparison of LULCC is very important for the management of natural resources and sustainable development, as it indicates the interaction between the environment and human beings in that region. Remote sensing techniques are often used as they significantly reduce the cost and time required for this task. Advances in remote sensing have made possible the rapid and effective acquisition and analysis of environmental degradation [1] caused by climate and GPP changes and carbon supply [3].

The contributions of remote sensing technology through the use of Modis sensors provide advances in studies aimed at characterizing the dynamics of vegetation cover and carbon on the earth's surface, making it possible to estimate both the loss of dioxide carbon to the atmosphere and the absorption of carbon through from GPP [4], [5], [6].

Therefore, it is believed that emissions induced by LULCC in Legal Amazon have increased over the last few years and this change can be identified and quantified through multispectral images from the Modis sensor and mathematical models [7]. Thus, the objective of this research was to detect the emissions induced by the LULCC in the Legal Amazon through multispectral images from the Modis sensor in the period 2009-2019.

2. MATERIAL AND METHODS

2.1. Study area

The Legal Amazon corresponds to the area of action of the Superintendence for the Development of the Amazon, delimited in accordance with Art. 2 of Law 124/2007. It has a surface of 5,015,067.75 km², corresponding to about 58.9% of the Brazilian territory [8]. In addition to containing 20% of the Savanna biome and a small part of the Pantanal biome, the region has the most extensive Brazilian biomes, the Amazon biome (Figure 1).

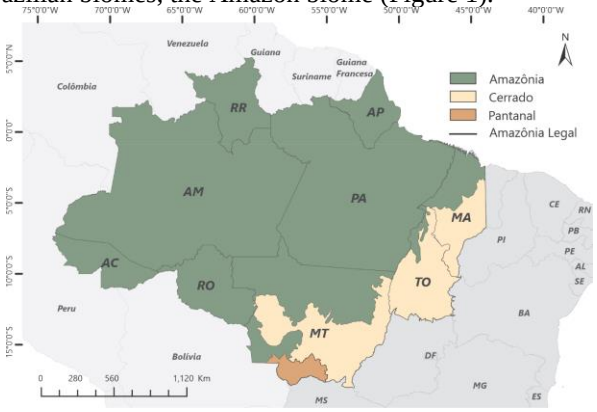

Figure 1. Map of the Legal Amazon and its biomes [8].

The climate in Legal Amazon is type "A", or tropical, in which the average monthly of 18 °C [9]; Three are the “Af” type (hot and rainy throughout the year), located from the northwest, the “Aw” type (tropical climate, with dry winter), between the south and east, and the “Am” type (humid or sub-humid tropical climate), from the northeast and south, in the transition between the others climates of Legal Amazon.

2.2. Land use and land cover change (LULCC)

To detect LULCC, the product MCD12Q1 of the Modis sensor was used [10]. The parameters of each LULC were calculated using JavaScript language as input in the Google Earth Engine platform. The algorithm that processes the product MCD12Q1 (V006 Global 500 m Land Cover Type Product) is the supervised decision tree. The surface cover scheme identifies 17 classes defined by the International Geosphere Biosphere Program (IGBP), which includes 11 classes of natural vegetation, 3 classes of urbanized plots and 3 classes of unvegetated soil [10].

The Type 1 classification was used, as it is the most complete classification and of interest in this research.

2.3. Gross primary production (GPP)

The product MYD17A2 related to GPP is based on the concept of efficiency of use of solar radiation by vegetation (ε). GPP is linearly related to absorbed photosynthetically active radiation (APAR) that is calculated as the product of incident photosynthetically active radiation (PAR), in the visible spectral range of 0.4 - 0.7 μm, assumed to be 45% of the total incident solar radiation, and the fraction of absorbed photosynthetically active radiation by vegetation cover (FPAR) [4], according to Equation 1:

$$GPP = \varepsilon \times PAR \times FPAR \quad (1)$$

The pixel values referring to the digital numbers of the Modis images (Kg C m^{-2}) were converted into biophysical values by multiplying by the scale factor 0.0001 [4]. The GPP values were transformed from the accumulated value every 8 days to average values every 8 days and converted from Kg C m^{-2} d^{-1} to annual averages, in g C m^{-2} $year^{-1}$. For daily GPP values, daily averages were performed within each month, with their respective accumulated values.

2.4. Flux of carbon dioxide index (CO_2flux)

The CO_2Flux index is used to measure the efficiency of the vegetation-related carbon sequestration process [5], [6]. For this, two vegetation indices are often used, the staggered Photosynthetic Vegetation Index (sPRI), which estimates the carotenoid pigments in leaves, indicating the rate of CO_2 storage in the leaves, and the NDVI, which demonstrates the vigor of photosynthetically active vegetation, which may be able to capture carbon sequestration absorptions [6], [11].

To estimate sPRI, the spectral band 3 (459-479 nm) and 4 (545-565 nm) were used. For NDVI, band 1 (620-670 nm) and 2 (841-876 nm) were used. The bands used were from the Modis sensor, product MOD09A. The spatial, temporal and radiometric resolution were of 500 m, 1 to 2 days and 12 bits, respectively. The CO_2Flux values were the results of the annual averages for the analyzed time series, obtained by multiplying NDVI and sPRI [11], corrected by the Turbulent Vortex Covariance method by data measured with sensors in micrometeorological towers, according to Santos' methodology [5], Equation 2:

$$CO_2Flux = -66.207 * (NDVI * sPRI) + 13.63 \quad (2)$$

The values of the CO_2Flux index were also tabulated to verify their maximum and minimum and their variation over the time series studied, analyzed monthly and annually.

2.5. Precipitation analysis by CHIRPS

In order to ascertain the regularities of precipitation over the time series (2009-2019), a CHIRPS dataset developed by the U.S. Geological Survey (USGS) and the Climate Hazards Group at the University of California, Santa Barbara were used. It was used in this study due to the lack of temporal data from *in situ* stations in Legal Amazon and because they have been available from 1981 to the present, with spatial resolution of 0.05° (±5.3 km) and monthly, pentadal and decadal temporal resolution for the globe.

The analysis was carried out with the descriptive statistics of the data, through maximums and minimums in the time series.

3. RESULTS AND DISCUSSION

3.1. Land use and land cover changes

The largest areas were for classes 2, 9, 10 and 8, greater than 3.30, 0.77, 0.42 and 0.21 in M km², respectively, for all years studied (Table 1). The class 15 was not observed.

Classes	1	2	3	4	5	6	7	8
2009	126	3374352	1	9371	2685	314	171	219487
2010	111	3363599	0	10976	2838	321	101	223691
2011	114	3356746	0	11236	2672	332	65	226821
2012	119	3351449	0	12162	2526	384	60	225837
2013	133	3346878	0	12592	2293	420	60	225740
2014	141	3341806	0	13785	2266	471	66	222678
2015	145	3332142	0	15043	2276	525	87	218875
2016	143	3320506	0	15357	2206	729	102	218150
2017	158	3318989	0	16228	2122	831	99	212146
2018	148	3311487	0	15607	1572	884	73	217815
2019	123	3307899	0	16282	1554	824	60	219498
Média	133	3338714	0	13513	2274	549	86	220976
Classes	**9**	**10**	**11**	**12**	**13**	**14**	**16**	**17**
2009	814410	427688	42969	46469	3214	761	119	76486
2010	814458	430814	43318	47846	3218	753	119	76460
2011	820451	424922	44032	50618	3222	775	115	76502
2012	828405	419508	44751	52641	3225	808	120	76630
2013	831246	418880	45303	54131	3228	838	121	76762
2014	829377	425726	45900	55250	3232	885	127	76915
2015	825110	440198	46546	56518	3234	893	140	76892
2016	821453	454674	47346	56951	3237	915	166	76687
2017	814680	466125	46820	59372	3241	868	178	76765
2018	792856	489266	47712	60108	3245	799	161	76891
2019	777735	504235	47932	61454	3250	668	142	76970
Média	815471	445640	45694	54669	3232	815	137	76724

Table 1. Annual area, in km², of each land use and land cover classes, between 2009 and 2019, for the Legal Amazon.

The class 2 was seen from the central-west region to the north of the Legal Amazon, occupying all western. This class was also the one that suffered the most losses over the time series, of 66,452.7 km² [1]. In the peripheral regions

from east to south of the Legal Amazon, large areas of classes 9, 10 and 8 were observed. These classes always appear adjacent to each other and is known as the arc of deforestation [7]. The main concerns are classes 2, 8, 9, 10 and 12, with a significant loss of area in the 1st to 3rd classes and consequent increases in the last two. The accumulated in 2009 for classes 2, 8, 9 and 10 was 67.28%, 4.38%, 16.24% and 8, 53%, respectively. For class 12 areas, an area of 46,468.91 km² (0.92%) was found. In 2019, at the end of the period studied, the accumulated for 2, 8, 9, 10, 9 and 12 was 65.96%, 4.38%, 15.51%, 10.05% and 1.22%, respectively, which proves the deforestation [2], [7].

The Figure 2 represents an area denominated Santo Antônio do Matupi, for the years 2009 (Figure 2A and 2C) and 2019 (Figure 2B and 2D), which aimed to demonstrate the changes in the use of forest areas for areas that have been extensively anthropized.

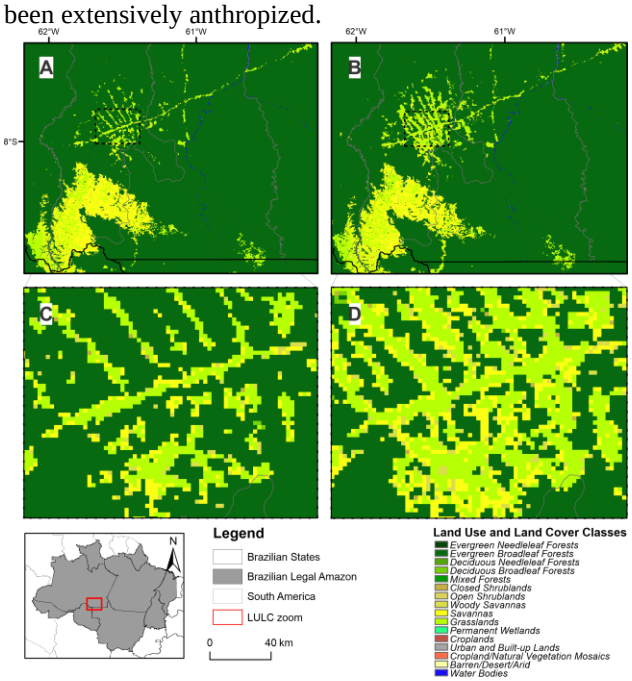

Figure 2. Land use and land cover change in Santo Antônio do Matupi region, from Manicoré city, in the State of Amazonas, for 2009 (A) to 2019 (B) and its expanded versions (C) and (D).

This location was especially chosen for presenting significant forest losses, mainly of class 2 and the increase of 9 and 10, for the deforestation. In this region, greater losses of primary forests were observed, with the most critical period of deforestation rates recorded between 2004 and 2018, when 63.28% of the area was converted to pastures [2]. The LULCC in Legal Amazon, with this deforestation, alter the balance between carbon absorption and emission, since forests are responsible for removing greenhouse gases from the atmosphere via sequestration and consequent absorption and storage of carbon, observed by the increase in gross primary production.

3.2. Gross primary production observations

The GPP values ranged from 1.42, in December 2015, to 9.00 gC m^{-2} d^{-1}, in June 2016. The averages were 5.9 gC m^{-2} d^{-1} for all years, with maximums for the last two years of 6.13 and 6.04 gC m^{-2} d^{-1}. Also, the sum of GPP was higher for the years 2018 and 2019, with values of 73.57 and 72.51 gC m^{-2}. The lowest value was for the year 2015.

Higher values of GPP were observed for the months from June to September in the time series, between 6.5 and 9 gC m^{-2} d^{-1} (Figure 3). On April and October, decreases in the GPP values were observed in all years studied, except for 2012 and 2016. In general, the minimums values were from March, April, September to November and the maximums from May to August (Figure 3).

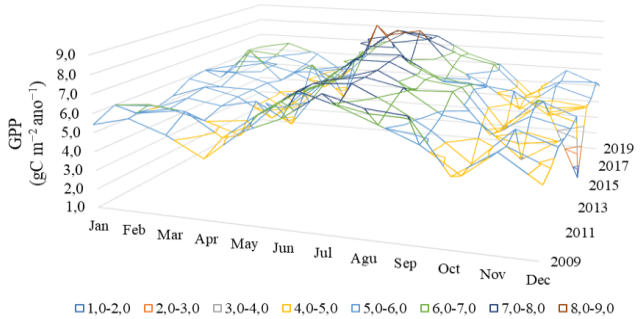

Figure 3. Daily GPP from Legal Amazon in 2009 to 2019.

Spatially, higher values of GPP were verified in the western, central and northern regions of Legal Amazon, while the lowest values were found in the peripheral region from east to south [3]. The maximum GPP values were found in the north, in regions close to the equator, with annual averages from 80.55 m^{-2} (2009) to 88.2 gC m^{-2} (2015), indicating higher carbon sequestration by absorption and storage. Mean values of carbon sequestration, between 40 and 44 m^{-2}, were observed in most of the north, central and west area.

3.3. Flux of carbon dioxide index (CO_2flux)

The values of the CO_2flux index ranged from -7.06, in June 2013, to 6.17 µmol m^{-2} s^{-1}, in February 2014. Both mean and sums values were negative, representing high CO_2 absorption. The monthly average was -2.78 µmol m^{-2} s^{-1}, and higher for 2015 and 2019 (Figure 4).

It is observed that for the month of January to March, positive values are observed, with emphasis on February 2014. After February, a decrease in CO_2flux values is observed, with a stabilization between the months of June and September, close to -5.5 µmol m^{-2} s^{-1}. A proportional inversion is observed in relation to the GPP values for the same period. Also, January to March were the months that had the highest values, regardless of the year, while June to August had the lowest values (Figure 4).

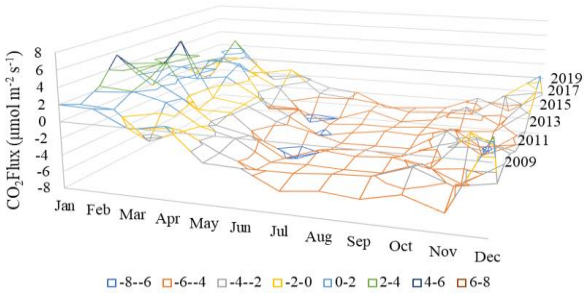

Figure 4. Mensal CO_2flux from Legal Amazon in 2009 to 2019.

As LULCC and GPP, lower CO_2flux values were found in the central and western regions of Legal Amazon, while higher values were observed in the peripheral regions from east to south and northeast. The highest absorption was identified for the year 2019, in areas identified as forests (class 2), and the maximum values were observed for water bodies (class 17), representing the lowest absorption of CO_2.

Values lower than -0.5 m^{-2} s^{-1} was obtained for forest areas (classes 1 to 5), indicating greater absorption for the entire time series analysed, and lower the further away from water bodies, mainly for class 2. Savanna areas, classes 6 to 9, oscillated between negative and positive values, remaining in a range of -0.51 and 2.58 µmol m^{-2} s^{-1} over the years. Agricultural fields and crops (class 12) obtained positive values, between 2.58 and 11.26 µmol m^{-2} s^{-1}, indicating lower carbon absorption and sequestration [11].

3.4. Precipitation analysis by CHIRPS

For all the years studied, the center, west and north of the Legal Amazon had the highest rainfall. The lowest rainfall was observed at the eastern to southeastern edges of the study area. The lowest annual accumulated rainfall was observed for 2015, with 1936.92 mm, followed by 2010, with 2046.34 mm, and 2016, with 2113.01 mm, years considered of extreme drought [1].

Regarding the months, June to October have the lowest rainfall, with July, August and September the most critical months, with less than 100 mm per month. December to April are months of high rainfall, above 200 mm per month. For all years, the months of January, February and/or March reached accumulated rainfall greater than 300 mm [9].

4. CONCLUSIONS

Our results show that forest areas, mainly for class 2, have higher values of GPP and accumulated precipitation and lower values of CO_2flux. The highest accumulated rainfall coincided with the areas classified as forests, while the lowest, with the savannas (classes 6 to 9), also encompassing the areas classified as grasslands (class 10).

The months from June to September present higher values of GPP and lower values of CO_2flux and accumulated precipitation and the opposite happened for the months of November to March.

5. REFERENCES

[1] L. E. O. C. Aragão, L. O. Anderson, M. G. Fonseca, T. M. Rosan, L. B. Vedovato, F. H. Wagner, C. V. J. Silva, C. H. L. Silva Junior, E. Arai, A. P. Aguiar, J. Barlow, E. Berenguer, M. N. Deeter, L. G. Domingues, L. Gatti, M. Gloor, Y. Malhi, J. A. Marengo, J. B. Miller, O. L. Phillips, and S. Saatchi, 21st Century drought-related fires counteract the decline of Amazon deforestation carbon emissions, *nature communications*, v. 9: p. 536, Dec. 2018.

[2] M. L. Duarte, J. A. P. de Sousa, A. L. de Castro, and R. W. Lourenço, Dynamics of land use in a rural settlement in the Brazilian Legal Amazon, *revista brasileira de ciências ambientais*, v. 56: pp. 375–384, Aug. 2021.

[3] C. A. da Silva Junior, M. Lima, P. E. Teodoro, J. F. de Oliveira-Júnior, F. S. Rossi, B. M. Funatsu, W. Butturi, T. Lourençoni, A. Kraeski, T. D. Pelissari, F. A. Moratelli, D. Arvor, I. M. dos S. Luz, L. P. R. Teodoro, V. Dubreuil, and V. M. Teixeira, Fires Drive Long-Term Environmental Degradation in the Amazon Basin, *remote sensing*, v. 14: p. 338, Jan. 2022.

[4] F. A. Heinsch, F. A. Heinsch, C. Milesi, W. M. Jolly, C. F. Bowker, J. S. Kimball, and R. R. Nemani, User ' s Guide NASA MODIS Land Algorithm Joseph Glassy, v. 4, 2003.

[5] C. V. B. SANTOS, Modelagem espectral para determinação de fluxo de CO2 em áreas de Caatinga preservada e em regeneração, Universidade Estadual de Feira de Santana., 2017.

[6] F. S. Rossi, C. A. da Silva Junior, J. F. de Oliveira-Júnior, P. E. Teodoro, L. S. Shiratsuchi, M. Lima, L. P. R. Teodoro, A. V. Tiago, and G. F. Capristo-Silva, 19-Year Remotely Sensed Data in the Forecast of Spectral Models of the Environment, *international journal of digital earth*, 2021.

[7] C. A. da Silva Junior, G. de Medeiros Costa, F. S. Rossi, J. C. E. do Vale, R. B. de Lima, M. Lima, J. F. de Oliveira-Junior, P. E. Teodoro, and R. C. Santos, Remote sensing for updating the boundaries between the brazilian Cerrado-Amazonia biomes, *environmental science & policy*, v. 101: pp. 383–392, 2019.

[8] IBGE, Amazônia Legal, 2021. [Online]. Available: https://www.ibge.gov.br/geociencias/cartas-e-mapas/mapas-regionais/15819-amazonia-legal.html?=&t=o-que-e. [Accessed: 24-Sep-2021].

[9] C. A. Alvares, J. L. Stape, P. C. Sentelhas, J. L. De Moraes Gonçalves, and G. Sparovek, Köppen's climate classification map for Brazil, *meteorologische zeitschrift*, v. 22: pp. 711–728, 2013.

[10] M. Friedl and D. Sulla-Menashe, MCD12Q1 MODIS/ Terra+Aqua Land Cover Tipo Anual L3 Global 500m SIN Grid V006, *NASA EOSDIS Processos Terrestres DAAC*, 2019. Available: https://lpdaac.usgs.gov/products/mcd12q1v006/. [Accessed: 22-Jun-2022].

[11] A. F. Rahman, J. A. Gamon, D. A. Fuentes, D. A. Roberts, and D. Prentiss, Modeling spatially distributed ecosystem flux of boreal forest using hyperspectral indices from AVIRIS imagery, *journal of geophysical research atmospheres*, v. 106: pp. 33579–33591, 2001.